Case Studies in Thermal Engineering 54 (2024) 104064

Contents lists available at ScienceDirect

Case Studies in Thermal Engineering

journal homepage: www.elsevier.com/locate/csite

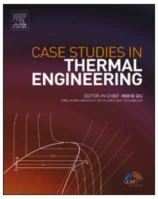

The effect of initial pressure on the thermal behavior of the silica aerogel/PCM/CuO nanostructure inside a cylindrical duct using molecular dynamics simulation

Yuanfei Gao[a,**], Ali Basem[b], S. Mohammad Sajadi[c], Dheyaa J. Jasim[d], Navid Nasajpour-Esfahani[e], Soheil Salahshour[f,g,h], Shadi Esmaeili[i], Sh. Baghaei[j,*]

[a] *School of Chemistry and Pharmaceutical Engineering, Nanyang Normal University, Nanyang, 473061, China*
[b] *Faculty of Engineering, Warith Al-Anbiyaa University, Karbala, 56001, Iraq*
[c] *Department of Nutrition, Cihan University-Erbil, Kurdistan Region, Iraq*
[d] *Department of Petroleum Engineering, Al-Amarah University College, Maysan, Iraq*
[e] *Department of Materials Science and Engineering, Georgia Institute of Technology, Atlanta, 30332, USA*
[f] *Faculty of Engineering and Natural Sciences, Istanbul Okan University, Istanbul, Turkey*
[g] *Faculty of Engineering and Natural Sciences, Bahcesehir University, Istanbul, Turkey*
[h] *Department of Computer Science and Mathematics, Lebanese American University, Beirut, Lebanon*
[i] *Faculty of Physics, Semnan University, P.O. Box: 35195-363, Semnan, Iran*
[j] *Department of Mechanical Engineering, Khomeinishahr branch, Islamic Azad University, Khomeinishahr, Iran*

ARTICLE INFO

Handling Editor: Huihe Qiu

Keywords:
Phase change materials
Silica aerogel
Initial pressure
Molecular dynamics simulation

ABSTRACT

Amidst escalating fuel expenses and growing concerns over greenhouse gas pollution, the adoption of renewable alternative energy sources has become increasingly imperative. In response, scientists are fervently dedicated to identifying energy-saving solutions that are readily adaptable. Notably, silica aerogels have demonstrated remarkable efficacy in temperature management under both hot and cold conditions, while phase change materials are renowned for their capacity to store thermal energy. The study examines the effect of initial pressure on the thermal performance of silica aerogel/PCM/CuO nanostructure in a cylindrical duct. This was investigated using MD simulations and the LAMMPS software. The study will investigate several elements, such as density, velocity, temperature patterns, heat flux, thermal conductivity, and charge time or discharge time of the simulated structure. According to the results, with an increase in the initial pressure, the maximum density increases from 0.0838 atom/Å^3 to 0.0852 atom/Å^{3,} and the maximum velocity decreases from 0.0091 Å/fs to 0.0081 Å/fs. Also, the findings show that, by increasing the initial pressure, the temperature decreases from 931.42 K to 895.63 K, and thermal conductivity and heat flux decrease to 1.56 W/m.K and 56.66 W/m^2 with increasing the initial pressure to 5 bar. Finally, the results show that charging time increases to 6.34 ns at 5 bar. The increase in charging time with increasing initial pressure may be attributed to the reduced mobility of particles within the structure as a result of the higher pressure. The findings of this study can help for a better understanding of energy-saving solutions, advanced thermal management systems, and the design of efficient energy storage technologies tailored to specific pressure-related operating conditions.

---

* Corresponding author.

** Corresponding author.

E-mail addresses: gaoyf19966@163.com (Y. Gao), shaghaieghbaghaie@yahoo.com (Sh. Baghaei).

https://doi.org/10.1016/j.csite.2024.104064
Received 15 October 2023; Received in revised form 2 January 2024; Accepted 21 January 2024

1. Introduction

Increasing levels of greenhouse gases and rising fuel costs caused a growing demand for cleaner energy alternatives [1]. Efficient energy storage methods that are easily adaptable to different forms pose difficulties for contemporary technology experts [2]. Energy storage plays a crucial role in regulating the energy reserves and consumption. Additionally, it assists in reducing expenses and conserving energy [3]. The concept of thermal energy storage involves the preservation of heat and cold to be utilized at a later time. The arrival of summer allows air conditioning units to convert cold winter air into a beneficial energy resource [4]. There are two primary methods to store heat: physical means, storing heat as either latent or sensible heat, and using chemical methods [5]. The ability of this method to adjust stages and maintain a constant temperature while storing a substantial amount of energy is genuinely intriguing [6]. The focus of this text is centered around a topic called phase change materials (PCMs). PCM refers to a form of substance that transforms one state into another. The forms of these objects are subject to alteration. Various changes can occur in substances, such as the transformation from a solid to a liquid, solid to a gas, or liquid to a gas, along with additional modifications [7]. PCM can store and release energy by transitioning from a solid state to a liquid state and vice versa [8]. Aerogel is a lightweight and highly porous solid material which are known for its low density, high porosity, and excellent thermal insulation capabilities, making it valuable for a wide range of applications. Aerogel maintains its properties throughout its transition from liquid to gas [9]. The energy storage capacity of PCMs can be significantly increased and prolonged by utilizing materials with numerous small air-filled compartments and efficient heat transfer properties. By learning techniques to save and preserve energy, they enhance their capacity in this field [10].

So far, various studies were done on the thermal behavior of PCMs, aerogels, and PCM/aerogel nanocomposites. For instance, Mahdavian et al. [11] focused on the thermal energy storage density and thermal conductivity of colloidal aerogels impregnated by PCMs. The model accurately predicts energy storage characteristics, demonstrating the potential for designing and optimizing energy storage materials for applications such as smart storage devices. Rostami et al. [12] reviewed the thermal performance and potential of 2D nanomaterial-based aerogels for encapsulating PCMs. By providing an overview of aerogel fabrication and their roles in composite PCMs, the review aims to stimulate interdisciplinary research and guide the design of advanced multifunctional 2 D aerogel-based composite PCMs, fostering breakthroughs in fundamental research and commercial applications. Patil et al. [13] investigated the thermal conductivity of reinforced silica aerogels with glass fibers. The results indicated that when silica is mixed with glass fibers, it creates materials with reduced thermal conductivity. Guingon et al. [14] investigated the effect of temperature changes on the thermal performance of PCM. According to the results, incorporating nanoparticles (NPs) enhances the thermal management and stability of the PCM's temperature. Li et al. [15] investigated the thermal behavior of paraffine PCMs incorporation of CuO NPs at different temperatures. The study discovered that adding CuO NPs to the simulated structures resulted in a more uniform change in the samples, and the melting time of the PCM decreased.

Previous studies show that various factors, such as temperature change, type of structure, addition of NPs, etc., affect the thermal behavior of nanostructures containing PCM and aerogels. However, so far, the effect of initial pressure on the thermal behavior of the silica aerogel/PCM/CuO nanostructure has not been investigated. Therefore, in the present study, a significant advancement in the field of initial pressure effect on the thermal behavior of the silica aerogel/PCM/CuO nanostructure within a cylindrical duct using molecular dynamics (MD) simulation. The innovative use of MD simulation techniques allows for a detailed investigation of properties such as maximum density, velocity, temperature, heat flux, thermal conductivity, and the charging and discharging time of the simulated structure at different initial pressures of 1, 2, 3, and 5 bar. This research holds great promise in providing valuable insights that can be applied to practical engineering applications, such as the design of advanced thermal management systems and energy storage devices. By addressing the complex interplay between initial pressure and thermal behavior, this study aims to fill a crucial gap in the current understanding of nanoscale thermal dynamics. The findings of this study are poised to contribute significantly to the existing body of knowledge in this domain and pave the way for future advancements in the field of thermal engineering and materials science.

2. Simulation method

MD simulation is beneficial for gaining insight into the mechanisms of large molecules in living organisms. By employing computer simulations, the MD method investigates the movement and interaction of particles within virtual models for a specified duration using the principles of physics.- Employing this method aids in improving our grasp of particle kinetics [16]. Scientists can gather information on particle movement in a system by employing a method known as MD simulation [17]. Newton's findings allow us to streamline the process by solving the equations that illustrate the motion of each part within the system. This technique enables us to replicate and gain comprehension of the motion and interaction between particles within a designated period [18]. In MD simulations, examining the relevance of the potential function and forces that govern particle interactions is essential. In other words, the potential function can be separated into bonded and non-bonded potentials. The total energy of a cluster of particles can be determined by considering their bonding and non-bonding properties [19].

$$E_{total} = E_{bonded} + E_{nonbonded} \tag{1}$$

The interaction between atoms, particularly when they are not bonded, creates various forms of energy. The total energy can be determined by analyzing the values acquired by applying Lennard-Jones potential functions. Our research will involve further investigation of these functions in the future [20,21]. The Lennard-Jones potential, a valuable mathematical tool, enhances our understanding of the interaction between two neutral particles or molecules [20,22]. To illustrate the Lennard-Jones potential function, Eq. (2) is commonly employed.

$$U_{LJ} = 4\varepsilon_{ij}\left[\left(\frac{\sigma_{ij}}{r_{ij}}\right)^{12} - \left(\frac{\sigma_{ij}}{r_{ij}}\right)^{6}\right] r < r_c \tag{2}$$

When particles are at a specific distance from each other, the ε_{ij} indicates the depth of their potential well." r_c" is a concise way of referring to the maximum distance commonly seen in computer-generated samples, typically about 12 Å. Selecting an accurate cut-off radius for every element in our simulations is essential [23–25]. When deciding, it is crucial to select and incorporate information about the area of expertise and consider the physical properties of the samples being examined. The quantities of gold, iron, silver, hydrogen, and carbon particles are depicted in Table 1.

By utilizing Table 1 and Eqs. (3) and (4), it can determine the values of "r" and gain insight into particle interactions. Here are the specific values that have been listed [28]:

$$\varepsilon_{ij} = \sqrt{\varepsilon_i \varepsilon_j} \tag{3}$$

$$\sigma_{ij} = \frac{\sigma_i + \sigma_j}{2} \tag{4}$$

Examining temperature, pressure, energy, and structure within ensembles aids in determining the stability of a system. Ensembles are commonly classified into three different groups: 1) microcanonical ensemble (NVE), 2) canonical ensemble (NVT), and 3) grand canonical ensemble (NPT) [29]. Multiple options are available to form a group that aligns with your preferences. Numerous methods are available in the microcanonical ensemble to maintain a constant temperature. Altering the velocity and ensuring a connection to a heat source are effective methods to maintain a consistent temperature. In addition, using Andersen and Nose-Hoover thermostats allows for temperature adjustment [30]. The simulations were utilized two distinct groups: the canonical and micro-canonical. Scientists in MD simulations utilize two different approaches to explore thermal properties. The first approach is the balance technique, whereas the second is called unbalanced dynamics. Thermal conductivity can be determined using the Green-Kubo formula's thermal calculations [31].

$$K = \frac{V}{3k_B T^2}\int_0^\infty dt\,(J(\tau).J(0)) \tag{5}$$

2.1. Simulation details

This research aimed to examine the influence of initial pressure on the behavior of silica aerogel and PCM inside a cylindrical channel in the presence of CuO NPs. Computer simulations were utilized by using a specific software, LAMMPS. This research employes computer software to simulate a space with dimensions of 300 × 300 × 100 $Å^3$. The tube contains a cylinder of silica aerogel, PCM, and CuO NPs located in the tube's center. PCM, silica aerogel, and CuO NPs can be modeled using the Avogadro software (See Fig. 1). The TIP3P model was used to model water molecules. The PCM and NPs structures are unified by employing the Packmol software. It is necessary to establish the boundary condition in all directions. Temperature changes are regulated utilizing the Nose-

Table 1
Parameters of the Lennard-Jones potential function for particles in MD simulations [26,27].

Particle type	σ (Å)	ε (kcal/mol)
Cu	3.495	0.005
O	3.500	0.06
C	3.851	0.105
H	2.886	0.044
S	4.035	0.274
H (H_2O)	0.4	0.046
O (H_2O)	3.1507	0.1521

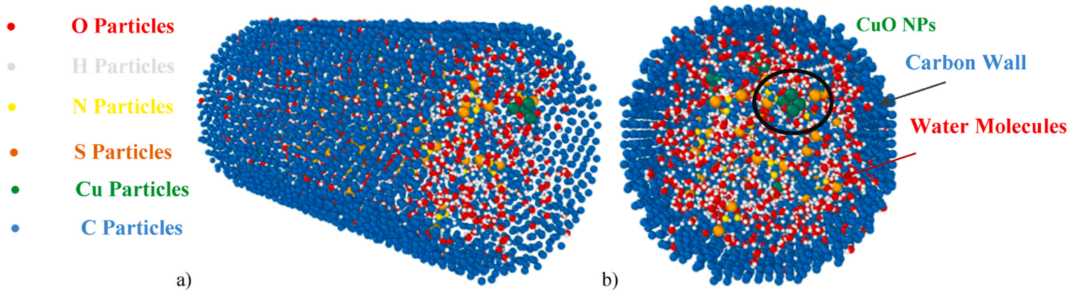

Fig. 1. Different views of the atomic structure of silica aerogel/PCM/CuO nanostructure from different views in the first step of MD simulations.

Hoover thermostat in computer simulations of atoms. Once the structure model is created, its stability is demonstrated using the NVT ensemble. Next, the ensemble changes to NPT, and the thermal properties such as maximum density, velocity, temperature, heat flux, thermal conductivity, and the charging and discharging time of the simulated structure at different initial pressures of 1, 2, 3, and 5 bar are investigated.

2.2. *The equilibration process*

The equilibration in samples will be studied by analyzing temperature and potential energy. The changes in temperature over a specific time are shown in Fig. 2. This visual representation showcases the atomic elements in a virtual form. The data indicates that temperature converges to 300 K after 10 ns. This convergence shows the adequacy of the simulation time.

Fig. 3 displays the change in the potential energy of the samples. Fig. 3 demonstrates that the potential energy of the analyzed sample converges to 276.46 kcal/mol after 10 ns. In the context of molecular dynamics simulations, the convergence of potential energy during the equilibration process is a critical indicator of the stability and adequacy of the simulation. When the potential energy converges, it signifies that the system has reached a state of equilibrium, where the intermolecular forces and interactions have balanced out. The system has settled into a stable configuration. This convergence demonstrates that the simulation has adequately captured the behavior of the system under study, and the selected simulation parameters, such as the potential function and simulation time, are appropriate for accurately representing the system's dynamics. It is an essential step in ensuring the reliability and accuracy of the simulation results.

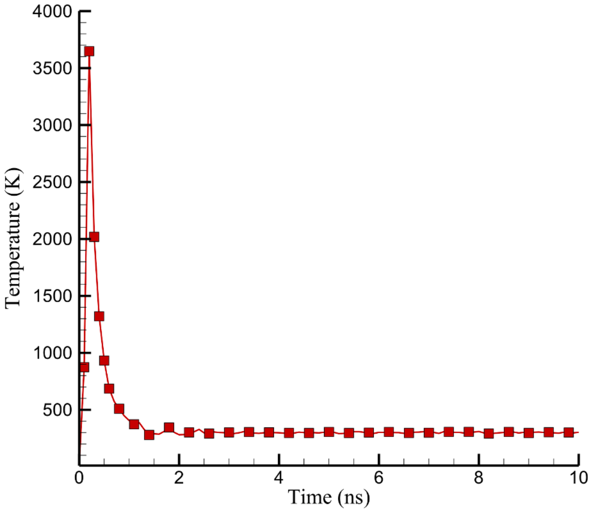

Fig. 2. Temperature changes concerning simulation time in the atomic structure of silica aerogel-paraffin in the presence of CuO NPs.

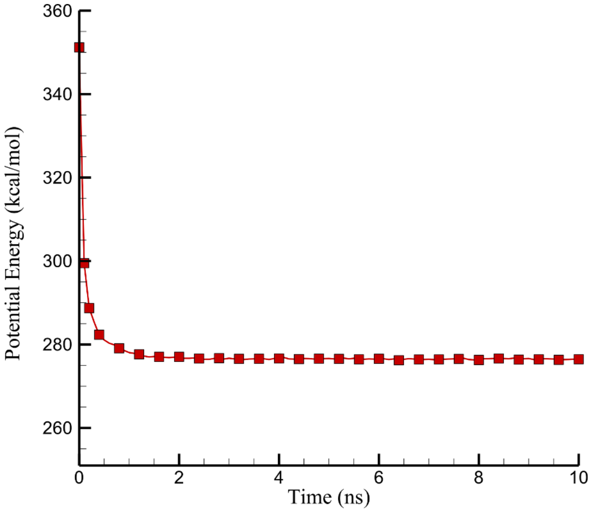

Fig. 3. Potential energy changes concerning simulation time in the atomic structure of silica-aerogel paraffin in the presence of CuO NPs.

Understanding the atomic structures' radial distribution function allows us to determine the arrangement and precise locations of atoms. Fig. 4 shows the spacing between oxygen atoms in water molecules in the studied sample once a state of equilibrium is reached.

3. Results and discussion

3.1. Results

The change in the sample's initial pressure significantly affects the evolution of the simulated samples. To check the effect of this factor, the initial pressure in the atomic samples is set equal to 1 bar, 2 bar, 3 bar, and 5 bar, and the atomic and thermal evolution of the samples is checked. Fig. 5 shows how the density of the simulated samples changes based on the initial pressure. Based on the findings, the maximum density has increased, rising from 0.0838 atom/Å^3 to 0.0852 atom/Å^3 with increasing pressure to 5 bar.

Fig. 6 shows the initial pressure's effect on the maximum velocity variations observed in the simulated samples. An increase in the initial pressure was resulted in a decrease in the maximum velocity of the sample.

Fig. 7 shows the observed temperature changes with increasing initial pressure. The data analysis revealed that the increase in initial pressure leads to a decrease in the maximum temperature. Fig. 7 reveals that as the pressure rises to 5 bar, the temperature decreases from 931.42 K to 895.63 K.

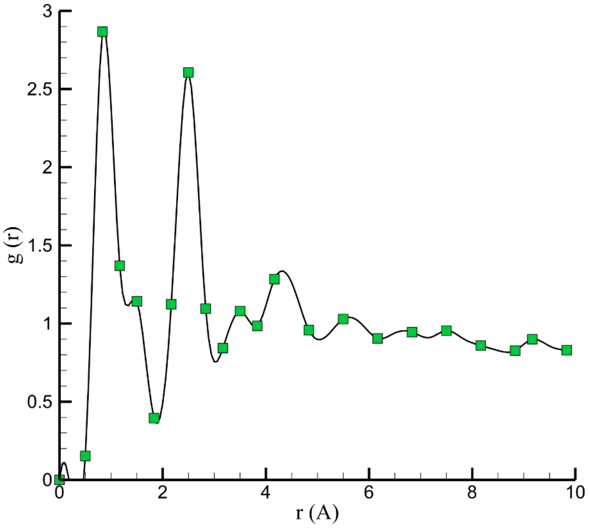

Fig. 4. Radial distribution function in the atomic structure of silica aerogel-paraffin in the presence of CuO NPs after equilibration in it.

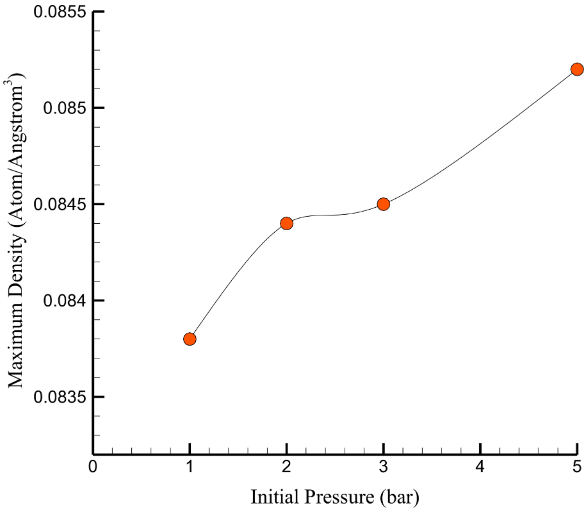

Fig. 5. Maximum density changes in the atomic structure of silica aerogel/paraffin/CuO at different initial pressures.

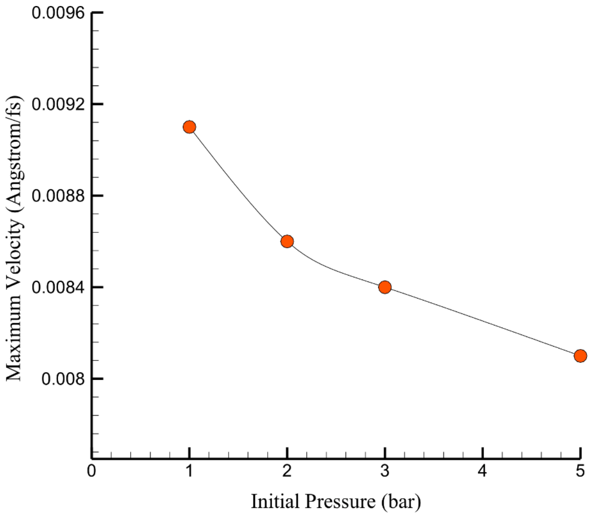

Fig. 6. Maximum velocity changes in the atomic structure of silica aerogel/paraffin/CuO at different initial pressures.

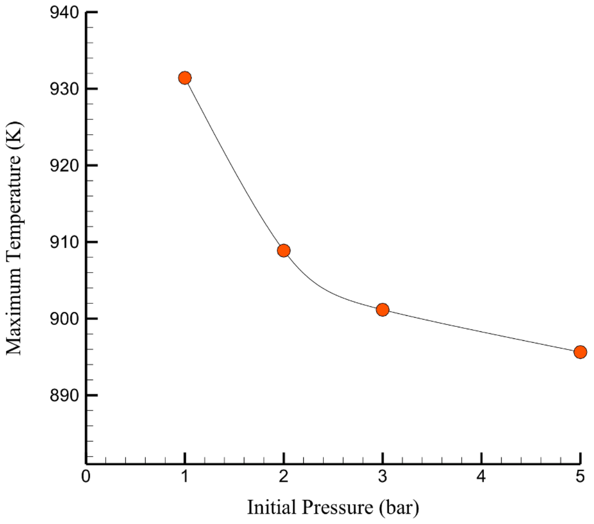

Fig. 7. Maximum temperature changes in the atomic structure of silica aerogel/paraffin/CuO at different initial pressures.

Fig. 8 shows the changes in thermal conductivity due to the increase in initial pressure. The obtained results showed that as the nanostructure's pressure increases, the nanostructure's thermal conductivity decreases from 1.62 to 1.56 W/m.K. Numerical results are reported in Table 2.

According to Fig. 9, the heat flux in the atomic sample decreases to 56.66 W/m^2 with increasing the initial pressure to 5 bar. Numerical results are reported in Table 2.

Fig. 10 shows the changes in charging time due to the increase in initial pressure. As the initial pressure increases, the charging time also increases. The results in Fig. 10 show an increase in charging time to 6.34 ns at 5 bar. On the other hand, increasing the pressure does not affect the discharge time of the structures, and the rate of this process remains constant in the thermal sample. According to Fig. 10. B, the discharge time remains at 8.27 ns.

3.2. Discussion

As the initial pressure is increased, the intermolecular spacing within the nanostructure decreases, leading to a higher packing density of atoms or molecules within the given volume. This compression effect results in a higher atomic density, as the atoms are forced to occupy a smaller space due to the applied pressure. Also, the results show that as the initial pressure of the structure is raised, the maximum velocity it can reach declines from 0.0091 Å/fs to 0.0081 Å/fs. The decrease in maximum velocity as the initial pressure of the structure is raised can be attributed to the increased intermolecular forces and reduced available space for movement within the structure. When the initial pressure is raised, the molecules within the structure experience greater compression, leading to a higher density of particles in a given volume. As a result, the interactions between molecules become stronger, causing a decrease in the overall mobility of the particles. Additionally, the higher initial pressure results in a more confined environment, limiting the

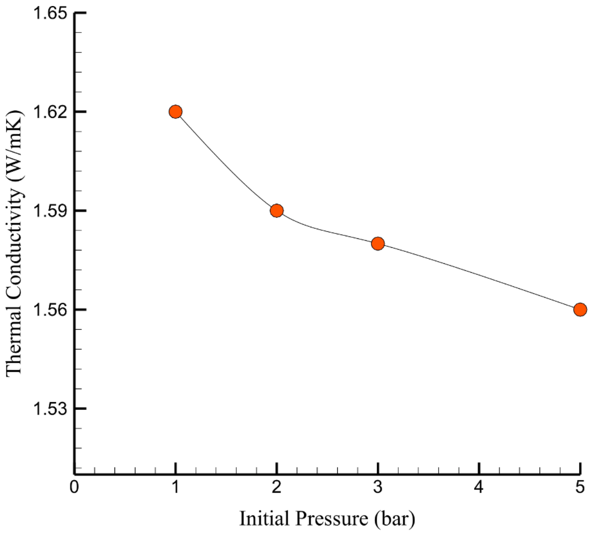

Fig. 8. Changing the thermal conductivity in the atomic structure of silica aerogel-paraffin-CuO at different initial pressures.

Table 2
Numerical outputs related to the atomic and thermal behavior of the atomic structure of silica-aerogel paraffin at different initial pressures.

Initial temperature (K)	Maximum density (atom/Ă^3)	maximum velocity (/fsÅ)	Maximum temperature (K)	Thermal conductivity (W/m.K)	Heat flux (W/m^2)	Charging time (ns)	Discharging time (ns)
1	0.0838	0.0091	931.42	1.62	60.88	6.16	8.29
2	0.0844	0.0086	908.88	1.59	60.03	6.25	8.28
3	0.0845	0.0084	901.16	1.58	58.61	6.31	8.27
5	0.0852	0.0081	895.63	1.56	56.66	6.34	8.27

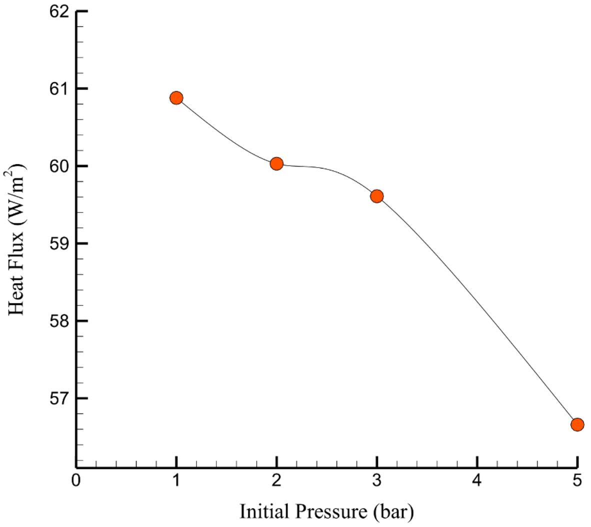

Fig. 9. Changing the heat flux in the atomic structure of silica aerogel-paraffin-CuO at different initial pressures.

available space for the molecules to move freely. This confinement restricts the maximum velocity that the particles can achieve, as they encounter greater resistance and reduced freedom of movement within the structure. In the following, the decrease in maximum temperature as the initial pressure of the structure is raised can be explained by the changes in the energy distribution and intermolecular interactions within the system. When the initial pressure is increased, the molecules within the structure are subjected to higher compression, leading to a higher density of particles in a given volume. This increased density results in a more significant interaction between the molecules, causing a reduction in the overall kinetic energy of the system. As a result of the increased intermolecular interactions and reduced available space for movement, the energy distribution within the system becomes more confined, leading to a decrease in the maximum temperature that the structure can reach. The higher initial pressure effectively limits the thermal energy that can be distributed among the particles, resulting in a lower maximum temperature for the system.

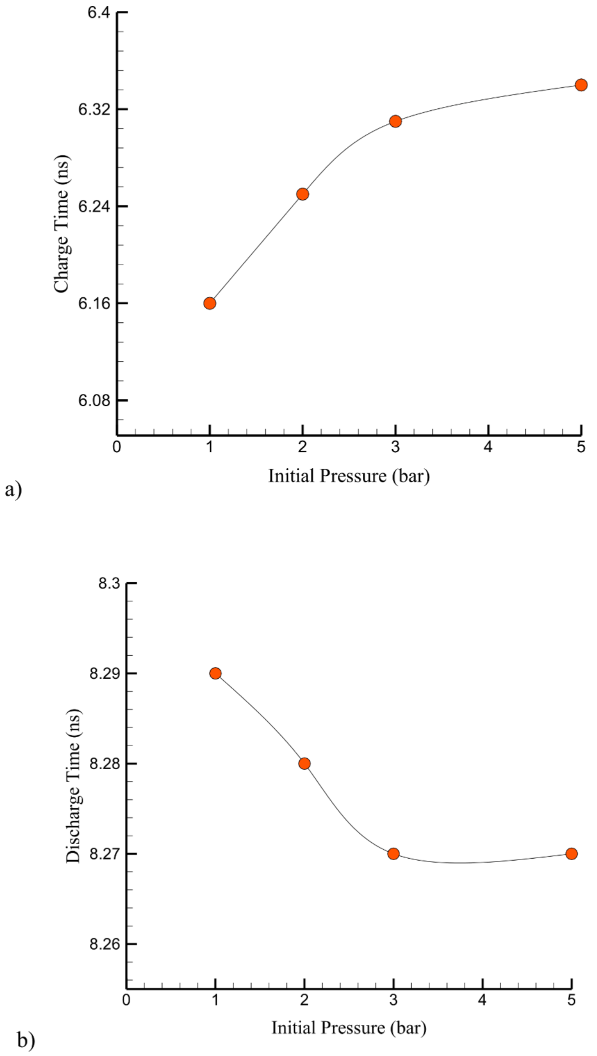

Fig. 10. Changing the a) charging and b) discharging time of the atomic structure of silica aerogel-paraffin-CuO at different initial pressures.

As mentioned before, as the initial pressure is increased to 5 bar, the average velocity of the atoms in the sample decreases. This decrease in velocity is a result of the higher density and closer proximity of the atoms due to the increased pressure. With reduced average velocity, the atoms have less kinetic energy to transfer heat through collisions, leading to a decrease in thermal conductivity. And the mean free path limits the ability of the atoms to transfer heat decrease, resulting in a lower thermal conductivity. Overall, the combination of reduced mean free path and lower atom velocity contributes to the observed decrease in thermal conductivity as the initial pressure increases. And the decrease in the heat flux in the atomic sample with increasing initial pressure to 5 bar can be attributed to the reduced thermal conductivity and increased intermolecular interactions within the system. When the initial pressure is raised, the molecules within the structure experience higher compression, leading to a greater density of particles in a given volume. This higher density and increased intermolecular interactions impede the flow of thermal energy through the system, resulting in a decrease in thermal conductivity. As a result, the transfer of heat energy becomes less efficient, leading to a reduction in the magnitude of the heat flux. The increased intermolecular interactions and reduced available space for movement restrict the mobility of thermal energy within the structure, leading to a lower heat flux.

Finally, the increase in charging time with increasing initial pressure may be attributed to the reduced mobility of particles within the structure as a result of the higher pressure. The increased pressure can lead to a decrease in the mobility of particles, slowing down their movement through the material. This reduced mobility results in a longer time required for the charging process to reach completion. On the other hand, increasing the pressure does not affect the discharge time of the structures. This may indicate that the discharge mechanism is less sensitive to the changes in pressure compared to the charging process.

4. Conclusion

This research aims to investigate the effect of initial pressure on the thermal behavior of the silica aerogel/PCM/CuO nanostructure within a cylindrical duct. To achieve this goal, computer simulations and the MD method were utilized. The equilibration results showed that the temperature and potential energy of the simulated structure reached 300 K. and 276.45 kcal/mol after 10 ns. This convergence shows the appropriateness of the selected pencil function and the adequacy of the simulation time. The results show that as the initial pressure of the structure is raised, the maximum velocity it can reach declines from 0.0091 Å/fs to 0.0081 Å/fs. The increase in initial pressure leads to a denser and more confined environment, resulting in stronger intermolecular forces and reduced space for movement, which collectively contribute to the observed decline in maximum velocity and temperature. Also, the results reveal that the thermal conductivity and heat flux in the atomic sample decreases to 1.56 W/m.K and 56.66 W/m^2 with increasing the initial pressure to 5 bar. The increase in initial pressure leads to a denser and more confined environment, which hinders the flow of thermal energy and reduces the overall thermal conductivity and heat flux within the system. The results of the present simulation can help to advance the development of more efficient thermal energy storage systems, contribute to heat transfer enhancement in electronics and aerospace applications, improve environmental control systems in enclosed environments, aid in the engineering of advanced insulation materials, and facilitate advancements in nanomaterial-based thermal management solutions.

CRediT authorship contribution statement

Yuanfei Gao: Investigation, Methodology, Project administration. **Ali Basem:** Resources, Software, Visualization. **S. Mohammad Sajadi:** Supervision, Validation, Writing – original draft. **Dheyaa J. Jasim:** Validation, Visualization, Writing – review & editing. **Navid Nasajpour-Esfahani:** Formal analysis, Investigation, Methodology. **Soheil Salahshour:** Formal analysis, Investigation, Methodology. **Shadi Esmaeili:** Formal analysis, Funding acquisition. **Sh. Baghaei:** Conceptualization, Data curation, Formal analysis.

Declaration of competing interest

The authors declare that they have no known competing financial interests or personal relationships that could have appeared to influence the work reported in this paper.

Data availability

No data was used for the research described in the article.

References

[1] S. Mekhilef, S. Siga, R. Saidur, A review on palm oil biodiesel as a source of renewable fuel, Renew. Sustain. Energy Rev. 15 (4) (2011) 1937–1949.
[2] J. Dai, R. Alvarado, S. Ali, Z. Ahmed, M.S. Meo, Transport infrastructure, economic growth, and transport CO2 emissions nexus: does green energy consumption in the transport sector matter? Environ. Sci. Pollut. Control Ser. 30 (14) (2023) 40094–40106.
[3] H. Garg, S. Mullick, V.K. Bhargava, Solar Thermal Energy Storage, Springer Science & Business Media, 2012.
[4] F.W. Schmidt, A.J. Willmott, Thermal Energy Storage and Regeneration, 1981.
[5] K. Muruganantham, Application of Phase Change Material in Buildings: Field Data vs, EnergyPlus simulation: Citeseer, 2010.
[6] A. Sharma, V.V. Tyagi, C. Chen, D. Buddhi, Review on thermal energy storage with phase change materials and applications, Renew. Sustain. Energy Rev. 13 (2) (2009) 318–345.
[7] M.A. Wahid, S.E. Hosseini, H.M. Hussen, H.J. Akeiber, S.N. Saud, A.T. Mohammad, An overview of phase change materials for construction architecture thermal management in hot and dry climate region, Appl. Therm. Eng. 112 (2017) 1240–1259.
[8] T.-C. Ling, C.-S. Poon, Use of phase change materials for thermal energy storage in concrete: an overview, Construct. Build. Mater. 46 (2013) 55–62.
[9] H. Weinläder, A. Beck, J. Fricke, PCM-facade-panel for daylighting and room heating, Sol. Energy 78 (2) (2005) 177–186.
[10] C. Li, D. Zhang, W. Ren, Phase change materials composite based on hybrid aerogel with anisotropic microstructure, Materials 14 (4) (2021) 777.
[11] F. Mahdavian, A. Allahbakhsh, D. Rodrigue, A.R. Bahramian, An analytical model for the energy storage potential of phase change materials supported by polymeric colloidal aerogels, J. Energy Storage 72 (2023) 108568.
[12] S. Rostami, A. Ghaffarkhah, A. Isari, S.A. Hashemi, M. Arjmand, 2D nanomaterial aerogels integrated with phase change materials: a comprehensive review, Materials Advances (2023).
[13] S.P. Patil, B.S. Bachhav, B. Markert, Thermal conductivity of glass fiber-reinforced silica aerogels using molecular dynamics simulations, Ceram. Int. 48 (2) (2022) 2250–2256.
[14] Q. Song, Y. Li, J. Xing, J. Hu, Y. Marcus, Thermal stability of composite phase change material microcapsules incorporated with silver nano-particles, Polymer 48 (11) (2007) 3317–3323.
[15] F. Li, A. Almarashi, M. Jafaryar, M.R. Hajizadeh, Y.-M. Chu, Melting process of nanoparticle enhanced PCM through storage cylinder incorporating fins, Powder Technol. 381 (2021) 551–560.
[16] J. Anwar, D. Zahn, Uncovering molecular processes in crystal nucleation and growth by using molecular simulation, Angew. Chem. Int. Ed. 50 (9) (2011) 1996–2013.
[17] M.N. Bergroth, M. Vogel, S.C. Glotzer, Examination of dynamic facilitation in molecular dynamics simulations of glass-forming liquids, J. Phys. Chem. B 109 (14) (2005) 6748–6753.
[18] S. Nose, Constant-temperature molecular dynamics, J. Phys. Condens. Matter 2 (S) (1990) SA115.
[19] D.C. Rapaport, The Art of Molecular Dynamics Simulation, Cambridge university press, 2004.
[20] J.E. Lennard-Jones, Cohesion, Proc. Phys. Soc. 43 (5) (1931) 461.
[21] P.G. Huray, Maxwell's Equations, John Wiley & Sons, 2011.
[22] T. Steinbrecher, D.L. Mobley, D.A. Case, Nonlinear scaling schemes for Lennard-Jones interactions in free energy calculations, J. Chem. Phys. 127 (21) (2007).
[23] S.-R. Yan, N. Shirani, M. Zarringhalam, D. Toghraie, Q. Nguyen, A. Karimipour, Prediction of boiling flow characteristics in rough and smooth microchannels using molecular dynamics simulation: Investigation the effects of boundary wall temperatures, J. Mol. Liq. 306 (112937) (2020) 112937, https://doi.org/10.1016/j.molliq.2020.112937.
[24] N.A. Jolfaei, N.A. Jolfaei, M. Hekmatifar, A. Piranfar, D. Toghraie, R. Sabetvand, S. Rostami, Investigation of thermal properties of DNA structure with precise atomic arrangement via equilibrium and non-equilibrium molecular dynamics approaches, Comput. Methods Programs Biomed. 185 (105169) (2020) 105169,

https://doi.org/10.1016/j.cmpb.2019.105169.

[25] M. Zarringhalam, H. Ahmadi-Danesh-Ashtiani, D. Toghraie, R. Fazaeli, Molecular dynamic simulation to study the effects of roughness elements with cone geometry on the boiling flow inside a microchannel, Int. J. Heat Mass Transf. 141 (2019) 1–8, https://doi.org/10.1016/j.ijheatmasstransfer.2019.06.064.

[26] H.J. Berendsen, J.R. Grigera, T.P. Straatsma, The missing term in effective pair potentials, J. Phys. Chem. 91 (24) (1987) 6269–6271.

[27] A.K. Rappé, C.J. Casewit, K. Colwell, W.A. Goddard III, W.M. Skiff, UFF, a full periodic table force field for molecular mechanics and molecular dynamics simulations, J. Am. Chem. Soc. 114 (25) (1992) 10024–10035.

[28] H. Berendsen, J. Grigera, T. Straatsma, The missing term in effective pair potentials, J. Phys. Chem. 91 (24) (1987) 6269–6271.

[29] D.C. Rapaport, The Art of Molecular Dynamics Simulation, Cambridge university press, 2004.

[30] D.C. Rapaport, The Art of Molecular Dynamics Simulation, Cambridge university press, 2004.

[31] M.S. Green, Markoff random processes and the statistical mechanics of time-dependent phenomena. II. Irreversible processes in fluids, J. Chem. Phys. 22 (3) (1954) 398–413.